

**Article type:** Communication

## **Histological and nuclear medical comparison of inflammation after haemostasis with non-thermal plasma and thermal coagulation**

Masashi Ueda\*, Daiki Yamagami, Keiko Watanabe, Kohei Sano, Hiroyuki Kimura, Asami Mori, Hideo Saji, Kenji Ishikawa, Masaru Hori, Hajime Sakakita, Yuzuru Ikehara, Shuichi Enomoto

---

M. Ueda, D. Yamagami, K. Watanabe, S. Enomoto  
Graduate School of Medicine, Dentistry, and Pharmaceutica Science, Okayama University,  
Okayama 700-8530, Japan  
E-mail: mueda@cc.okayama-u.ac.jp

K. Sano, H. Kimura, H. Saji  
Graduate School of Pharmaceutical Sciences, Kyoto University, Kyoto 606-8501, Japan

H. Kimura, A. Mori  
Radioisotope Research Center of Kyoto University, Kyoto 606-8501, Japan

K. Ishikawa, M. Hori  
Graduate School of Engineering, Nagoya University, Nagoya, 464-8603, Japan

H. Sakakita, Y. Ikehara  
National Institute of Advanced Industrial Science and Technology, Tsukuba, 305-8568, Japan

S. Enomoto  
Next-Generation Imaging Team, RIKEN Center for Life Science Technologies, Kobe 650-  
0047, Japan

---

### **Abstract**

The objective of this study is to examine the invasiveness of haemostasis by non-thermal plasma (NTP) compared with haemostasis by thermal coagulation (TC). The inflammation recovery process after haemostasis by TC and NTP was compared by using histological methods and nuclear medical molecular imaging. The necrotic areas in the NTP group disappeared after 5 days, whereas they remained 15 days after haemostasis in the TC group. The accumulation of 2-deoxy-2-fluoro-<sup>18</sup>F-D-glucopyranose (<sup>18</sup>F-FDG), which reflects

the existence of inflammatory cells, was higher in the TC group than in the NTP group on day 15. Thus, this study indicates that haemostasis by NTP is less inflammatory than TC. This report is the first to evaluate inflammation that occurred after haemostasis with medical devices noninvasively.

## Introduction

Plasma is a mixture of ionized molecules, radicals, and electrons that is generated by intense electromagnetic fields. Recently, techniques to generate non-thermal plasma (NTP) at atmospheric pressure have been developed. There are several medical applications of NTP, including in blood coagulation, wound healing, bacterial inactivation, and cancer treatment.<sup>[1-5]</sup> Bleeding from vessels in clinical practice is controlled by cauterization with a thermal coagulator (TC). However, the mechanical contact and heat produced by the TC injures tissues and causes long-lasting inflammation and postoperative problems.<sup>[6,7]</sup> Haemostasis by NTP may overcome these issues because it is a noncontact method and the gas temperature of NTP is close to the ambient temperature. To establish NTP haemostasis as a common medical practice, it is necessary to elucidate a detailed profile of inflammation following NTP haemostasis.

Nuclear medical molecular imaging is a procedure to visualize the distribution of radiopharmaceuticals noninvasively by using an imaging modality such as positron emission tomography (PET). Since a target protein that specifically binds to and/or metabolizes radiopharmaceuticals regulates their accumulation, this technique can evaluate the amount and localization of the target protein's expression. Thus, nuclear medical molecular imaging contributes to reveal physiological functions and disease-related changes of the target proteins. In fact, many diseases, such as Alzheimer's disease, cancer, and myocardial infarction can be detected by nuclear medical molecular imaging.<sup>[8-10]</sup> Furthermore, PET imaging has been used recently to monitor and/or predict the efficacy of drug treatment, both in preclinical and clinical settings.<sup>[11,12]</sup> Therefore, we applied this concept to evaluate the severity of inflammation after haemostasis either by NTP or by TC.

Among radiopharmaceuticals, 2-deoxy-2-fluoro-<sup>18</sup>F-D-glucopyranose (<sup>18</sup>F-FDG) is one of the most commonly used in the world. Because it is an analogue of glucose, cells take up <sup>18</sup>F-FDG instead of glucose. Therefore, areas where many and/or active cells exist, such as

inflammatory sites, can be visualized by  $^{18}\text{F}$ -FDG.<sup>[13]</sup> This study aimed to compare inflammation and the healing process after haemostasis with NTP or TC by histological analysis and  $^{18}\text{F}$ -FDG imaging, and revealed that NTP haemostasis was less invasive. This study is a first challenge to evaluate inflammation that occurs after haemostasis with medical devices noninvasively.

## **Experimental Section**

### **Plasma equipment and experimental setup**

An NTP device was used as previously described.<sup>[14,15]</sup> Helium was used as the working gas. While He gas was flowing, the peak to peak voltage applied to the electrode was 6.1 kV for the plasma production. The line averaged electron density in the plasma source was  $8 \times 10^{14} \text{ cm}^{-3}$ , and the effective current to the target was 0.37 mA. The flow rate of He gas was set at two standard litres per minute, and the distance between the tip of the plasma jet and samples was fixed at 10 mm.

### **Surgical operation**

Animal studies were conducted in accordance with our institutional guidelines, and the Okayama University Animal Care Committee approved the experimental procedures. Male ICR mice ten weeks of age were purchased from Japan SLC, Inc. (Hamamatsu, Japan) and maintained at a constant ambient temperature with a 12-h light/dark cycle and free access to food and water. The mice were anesthetized by intraperitoneal injection of sodium pentobarbital (10 mg/kg) and then placed in a supine position. The liver was exposed and cut (length: 20 mm, depth: 3 mm) using a surgical mess, and blood from the wound was stopped using either a bipolar TC (Micro-3E, Mizuho Ika Kogyo Co., Ltd., Chiba, Japan) or an NTP. The abdominal incision was closed with sutures after completing haemostasis. In the sham-

operated group, the liver was exposed, left intact, and then irradiated with NTP for the same duration as the NTP group. The mice were individually returned to their cages and left to recover until the experiments.

### **Histological analysis**

For the histological assessment, the mice (n = 3 for each time point) were euthanized 1, 5, and 15 days after the surgical operation, and the livers were removed. After taking photographs of the livers, they were embedded in Optimal Cutting Temperature compound (Sakura Finetek Japan Co., Ltd., Tokyo, Japan) and frozen on dry ice. Tissue sections (5- $\mu$ m thick) were prepared by using a cryomicrotome (CM1850 Cryostat; Leica Microsystems, Wetzlar, Germany) and mounted on MAS-coated glass slides (Matsunami Glass Ind., Ltd., Osaka, Japan). The tissue sections were fixed with 4% paraformaldehyde/phosphate-buffered saline (PBS) and then stained with haematoxylin and eosin (HE). Changes in histological morphology were observed with a microscope (BZ-9000; Keyence Corporation, Osaka, Japan).

### **Autoradiography**

Autoradiography was performed 5 and 15 days after surgery in both the TC and NTP groups (n = 5–7). The mice were intravenously injected with  $^{18}\text{F}$ -FDG (11.4–41.9 MBq). At 2 h after injection, the mice were euthanized, and the livers were removed and frozen. The frozen liver samples were sliced into 20- $\mu$ m thick sections with the cryomicrotome (CM1900 Cryostat). The sections were exposed to imaging plates (BAS-SR; Fuji Photo Film, Tokyo, Japan) for 1 h. Autoradiograms of these sections were obtained with a BAS5000 scanner (Fuji Photo Film).<sup>[16]</sup> The intensity and area of  $^{18}\text{F}$ -FDG accumulation in the haemostasis sites were quantified using a dedicated software (Image Gauge ver. 3.1; Fuji Photo Film).<sup>[17]</sup>

## **<sup>18</sup>F-FDG PET/CT**

PET and X-ray computed tomography (CT) were performed 5 and 15 days after surgery in both the TC and NTP groups (n = 2). The mice were intravenously injected with <sup>18</sup>F-FDG (17.5–44.3 MBq). At 2 h after injection, the mice were imaged for 10 min by using Triumph LabPET12/SPECT4/CT (TriFoil Imaging Inc., Chatsworth, CA, USA) under 2.5 % isoflurane anaesthesia.<sup>[18]</sup> Coincident data were collected for 511-keV gamma rays with an energy window of 250–650 keV. PET images were reconstructed by using a three-dimensional ordered-subset expectation maximization algorithm (20 iterations, 4subsets). After the PET imaging, a CT scan was performed for 5 min. The tube voltage and current were set at 60 kV and 320  $\mu$ A, respectively.

PET and CT images were fused, and the accumulated radioactivity in the volumes of interest (VOIs) was quantified by a dedicated software (PMOD software ver. 3, PMOD Technologies Ltd., Zurich, Switzerland). Spheroidal VOIs on the surface of the liver were set to be the same size (20 x 3 x 4 mm) in both groups. The VOI size was based on the maximum lesioned area to avoid underestimation caused by the partial volume effect.

## **Statistical Analyses**

The statistical difference between the two groups was evaluated by a Student's *t*-test. Differences were considered significant when the P value was less than 0.05.

## **Results and Discussion**

### **Histological analysis**

Figure 1 shows macroscopic images of the liver treated with TC or NTP. Large lesioned areas were observed in the TC group and the areas still existed 15 days after surgery.

In contrast, the lesioned areas in the NTP group were much smaller than in the TC group, and the areas had disappeared by day 15. The results from the HE-stained sections agreed with the macroscopic observations. Large necrotic areas were observed in the TC group, and the areas remained on day 15 (Figure 2, arrows). On the other hand, in the NTP group, although a small necrotic area existed on day 1, it disappeared by day 5, and inflammatory cells had migrated instead (Figure 2, arrowhead). On day 15, many inflammatory cells surrounded the necrotic area in the TC group, but the migrated inflammatory cells had almost completely disappeared in the NTP group. In general, wound healing starts from haemostasis and haemostasis initiates the inflammatory process, i.e., the recruitment of neutrophils and macrophages. After the inflammatory phase, proliferation and remodelling of tissues occur and the wound healing process is completed.<sup>[19]</sup> Thus, the histological analysis indicated that the wound healing process after NTP haemostasis was faster than after TC haemostasis. When the intact liver was irradiated with NTP or He, no necrotic area was observed (Figure 2). Therefore, the necrotic area observed on day 1 in the NTP haemostasis group was not caused by NTP irradiation.

### **Autoradiography**

It has been reported that the expression of neutrophils and macrophages correlates with the inflammatory reaction.<sup>[20]</sup> Since  $^{18}\text{F}$ -FDG was taken up by neutrophils and macrophages,<sup>[21]</sup> we used  $^{18}\text{F}$ -FDG to evaluate the severity of the inflammation that occurred after haemostasis with TC or NTP. Representative autoradiograms are shown in Figure 3A. The accumulation sites of  $^{18}\text{F}$ -FDG are indicated by arrows and correspond to the haemostasis sites (data not shown). Quantitative analyses revealed that the intensity of radioactivity accumulation was similar in both groups (Figure 3B). In contrast, the area of radioactivity accumulation in the NTP group was significantly smaller than that in the TC group (Figure 3C). These findings suggest that although the severity of inflammation that occurred in the

haemostasis sites is similar regardless of haemostasis methods, the inflammatory area in the NTP group disappeared faster than in the TC group. The inflammatory process can be divided into two phases: an early phase with neutrophil recruitment and a late phase with macrophage migration.<sup>[19]</sup> However, in this study, it was unclear which phases of inflammation occur after haemostasis with TC and NTP, because <sup>18</sup>F-FDG accumulated in both cells. Immunohistochemical analyses for neutrophils and macrophages will answer that question.

### **PET/CT imaging**

Finally, a preliminary PET evaluation was performed. Figure 4 shows the representative PET/CT images. Since the <sup>18</sup>F ion that is attributable to metabolism of <sup>18</sup>F-FDG in vivo accumulates in bone<sup>[22]</sup>, the vertebrae were clearly visualized in all mice (Figure 4, circles). On day 5, prominent radioactivity accumulated in the laparotomy wound, and it was difficult to compare the radioactivity accumulated in the liver in the two groups. On the other hand, on day 15, much more radioactivity accumulated in the liver of the TC group than the NTP group (Figure 4, arrowheads). The results of the quantitative analysis agreed with visual evaluation. The standardized uptake values that represent the radioactivity concentration in tissues of interest<sup>[23]</sup>, the liver in this case, were 0.27 and 0.30 in the TC group and 0.19 and 0.21 in the NTP group. Although the statistical difference could not be evaluated due to the limited number of mice examined, <sup>18</sup>F-FDG accumulation in the NTP group was approximately 2/3 of the accumulation in the TC group. This finding suggests that haemostasis with NTP is less invasive than haemostasis with TC.

### **Conclusion**

In comparison, NTP haemostasis resulted in earlier clearance of both inflammatory cell infiltration and <sup>18</sup>F-FDG accumulation at the haemostasis site than TC haemostasis. Thus,

this study indicates that NTP haemostasis is associated with a shorter period of inflammation than TC haemostasis. We have noninvasively succeeded in evaluating inflammation that occurred after haemostasis with medical devices for the first time.

Acknowledgements: The authors are grateful to Okayama Medical Innovation Center for their assistance with image analyses. This study was supported in part by a Grant-in-Aid for Scientific Research on Innovative Areas (Research in a proposed research area), Plasma Medical Innovation (KAKENHI No. 25108508, 15H00895) from the Japan Society for the Promotion of Science.

Keywords: haemostasis; imaging; inflammation; non-thermal plasma; positron emission tomography

## References

- [1] M.G. Kong, G. Kroesen, G. Morfill, T. Nosenko, T. Shimizu, J. van Dijk, J.L. Zimmermann, *New J Phys* **2009**, *11*, 115012.
- [2] D. Dobrynin, G. Fridman, G. Friedman, A. Fridman, *New J Phys* **2009**, *11*, 115020.
- [3] J. Heinlin, G. Morfill, M. Landthaler, W. Stolz, G. Isbary, J.L. Zimmermann, T. Shimizu, S. Karrer, *J Dtsch Dermatol Ges* **2010**, *8*, 968.
- [4] J. Heinlin, G. Isbary, W. Stolz, G. Morfill, M. Landthaler, T. Shimizu, B. Steffes, T. Nosenko, J.L. Zimmermann, S. Karrer, *J Eur Acad Dermatol* **2011**, *25*, 1.
- [5] M. Yousfi, N. Merbahi, A. Pathak, O. Eichwald, *Fund Clin Pharmacol* **2014**, *28*, 123.
- [6] G.M. Boland, R.J. Weigel, *J Surg Res* **2006**, *132*, 3.
- [7] B. Kraemer, M. Scharpf, C. Planck, C. Tsaousidis, M.D. Enderle, A. Neugebauer, K. Kroeker, F. Fend, S. Brucker, R. Rothmund, *Fertil Steril* **2014**, *102*, 1197.
- [8] C.H. Lyoo, M. Ikawa, J.S. Liow, S.S. Zoghbi, C.L. Morse, V.W. Pike, M. Fujita, R.B. Innis, W.C. Kreisl, *J Nucl Med* **2015**, *56*, 701.
- [9] M. Eiber, T. Maurer, M. Souvatzoglou, A.J. Beer, A. Ruffani, B. Haller, F.P. Graner, H. Kubler, U. Haberhorn, M. Eisenhut, H.J. Wester, J.E. Gschwend, M. Schwaiger, *J Nucl Med* **2015**, *56*, 668.
- [10] R.R. Packard, S.C. Huang, M. Dahlbom, J. Czernin, J. Maddahi, *J Nucl Med* **2014**, *55*, 1438.
- [11] R.M. Connolly, J.P. Leal, M.P. Goetz, Z. Zhang, X.C. Zhou, L.K. Jacobs, J. Mhlanga, J.H. O, J. Carpenter, A.M. Storniolo, S. Watkins, J.H. Fetting, R.S. Miller, K. Sideras, S.C. Jeter, B. Walsh, P. Powers, J. Zorzi, J.C. Boughey, N.E. Davidson, L.A. Carey, A.C. Wolff, N. Khouri, E. Gabrielson, R.L. Wahl, V. Stearns, *J Nucl Med* **2015**, *56*, 31.
- [12] H.G. Keen, S.A. Ricketts, J. Maynard, A. Logie, R. Odedra, A.M. Shannon, S.R. Wedge, S.M. Guichard, *Mol Imaging Biol* **2014**, *16*, 421.

- [13] K. Higashikawa, N. Akada, K. Yagi, K. Watanabe, S. Kamino, Y. Kanayama, M. Hiromura, S. Enomoto, *Biochem Biophys Res Commun* **2011**, *410*, 416.
- [14] H. Sakakita, Y. Ikehara, *Plasma Fusion Res* **2010**, *5*, S2117.
- [15] Y. Ikehara, H. Sakakita, N. Shimizu, S. Ikehara, H. Nakanishi, *J Photopolym Sci Tec* **2013**, *26*, 555.
- [16] M. Ueda, T. Fukushima, K. Ogawa, H. Kimura, M. Ono, T. Yamaguchi, Y. Ikehara, H. Saji, *Biochem Biophys Res Commun* **2014**, *445*, 661.
- [17] M. Ueda, Y. Iida, A. Tominaga, T. Yoneyama, M. Ogawa, Y. Magata, H. Nishimura, Y. Kuge, H. Saji, *Br J Pharmacol* **2010**, *159*, 1201.
- [18] M. Ueda, H. Hisada, T. Temma, Y. Shimizu, H. Kimura, M. Ono, Y. Nakamoto, K. Togashi, H. Saji, *Mol Imaging Biol* **2015**, *17*, 102.
- [19] J.M. Reinke, H. Sorg, *Eur Surg Res* **2012**, *49*, 35.
- [20] J.B. Watelet, P. Demetter, C. Claeys, P. Van Cauwenberge, C. Cuvelier, C. Bachert, *Histopathology* **2006**, *48*, 174.
- [21] D. Saha, K. Takahashi, N. de Prost, T. Winkler, M. Pinilla-Vera, R.M. Baron, M.F.V. Melo, *Mol Imaging Biol* **2013**, *15*, 19.
- [22] H. Jadvar, B. Desai, P.S. Conti, *Semin Nucl Med* **2015**, *45*, 58.
- [23] C. Lasnon, A.E. Dugue, M. Briand, C. Blanc-Fournier, S. Dutoit, M.H. Louis, N. Aide, *Mol Imaging Biol* **2015**, *17*, 403.

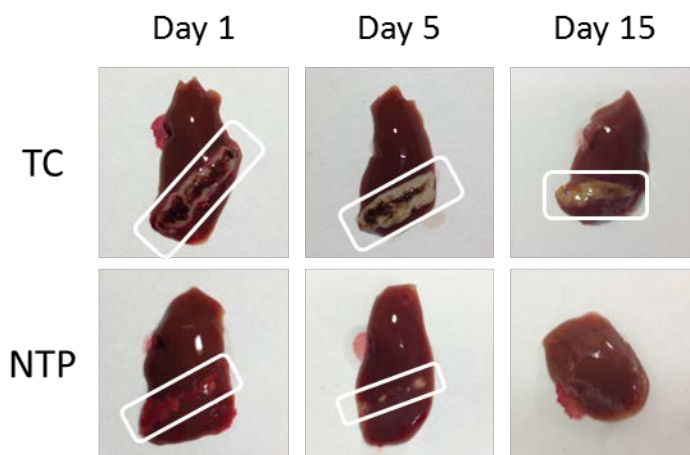


*Figure 1.* Representative macroscopic images of the livers. Lesioned areas that resulted from different haemostasis treatments (TC or NTP) are highlighted by white boxes. Data were obtained from 3 mice.

TC, thermal coagulator; NTP, non-thermal plasma.

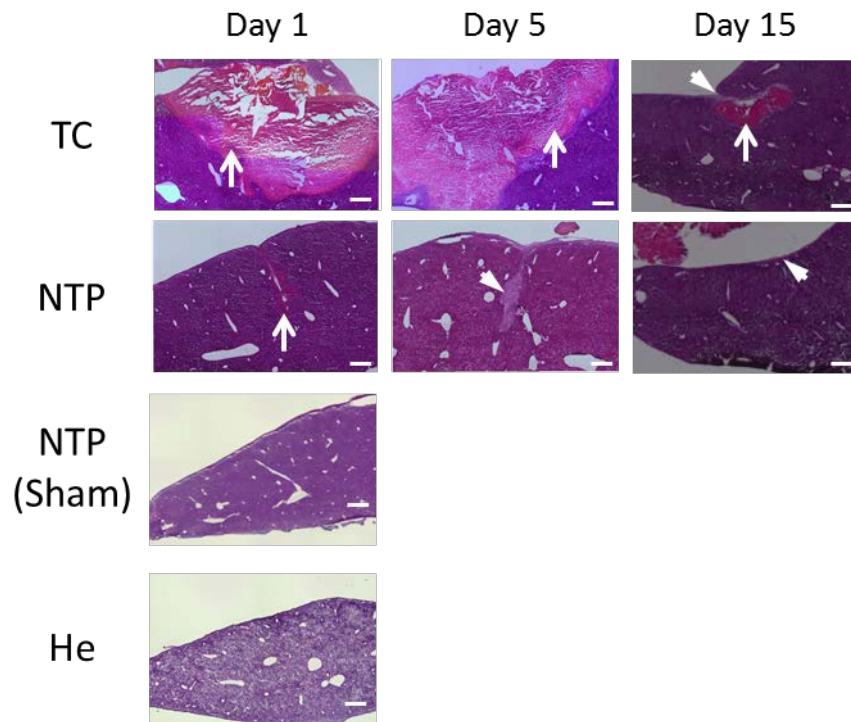


*Figure 2.* Liver sections stained with haematoxylin-eosin. The arrows and arrowheads indicate the necrotic areas and areas with accumulated inflammatory cells, respectively. Data were obtained from 3 mice.

TC, thermal coagulator; NTP, non-thermal plasma; Scale bars, 500  $\mu$ m.

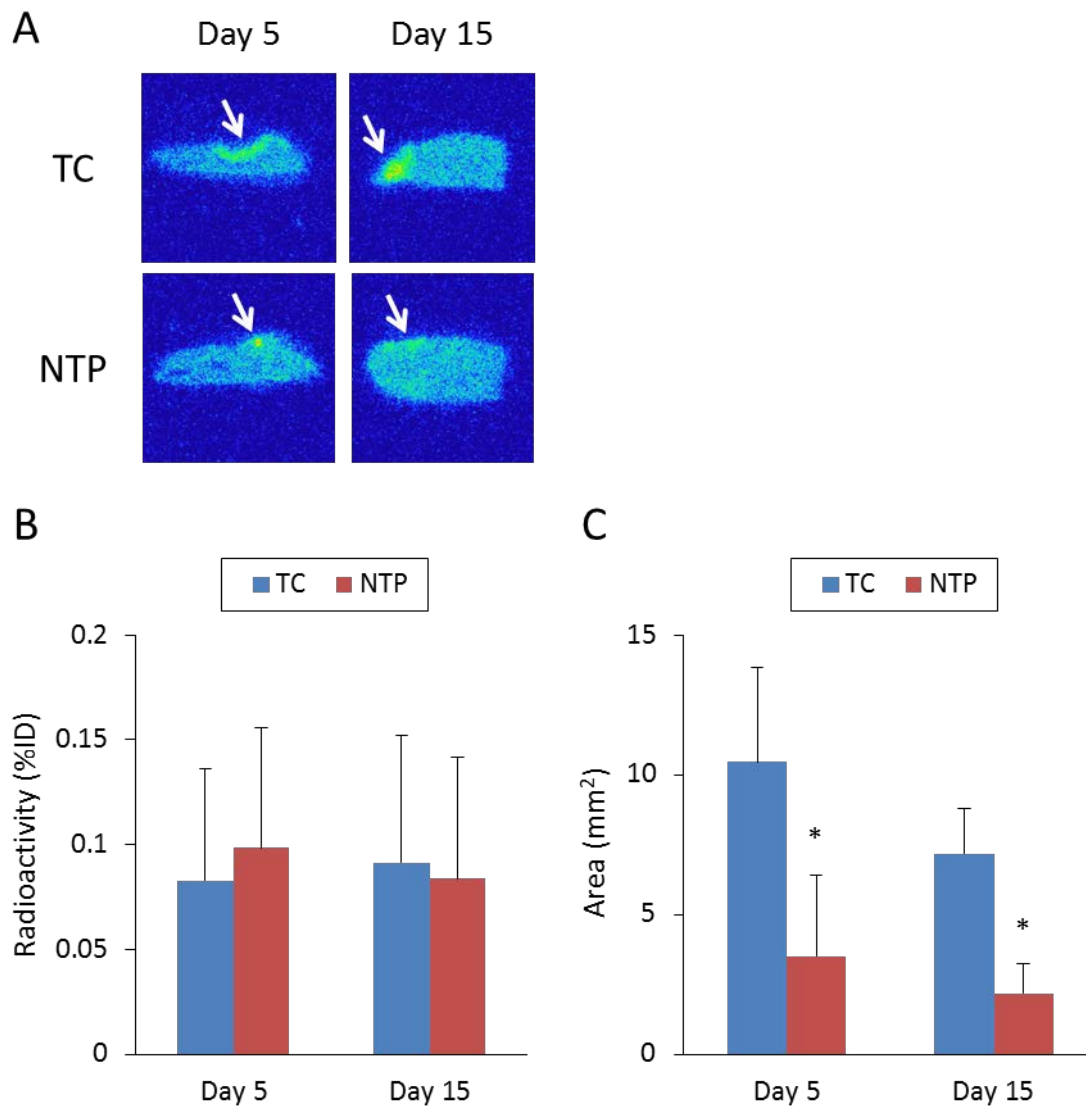


*Figure 3.* (A) Representative autoradiograms of liver sections. The areas with accumulated <sup>18</sup>F-FDG are indicated by the arrows. (B) The intensity of radioactivity accumulation in the haemostasis site with NTP and TC. Columns and bars represent the mean and standard deviation (n = 5–7), respectively. (C) The area of radioactivity accumulation in the haemostasis sites with NTP or TC. Columns and bars represent the mean and standard deviation (n = 5–7, \**P* < 0.05), respectively.

TC, thermal coagulator; NTP, non-thermal plasma; %ID, percent injected dose.

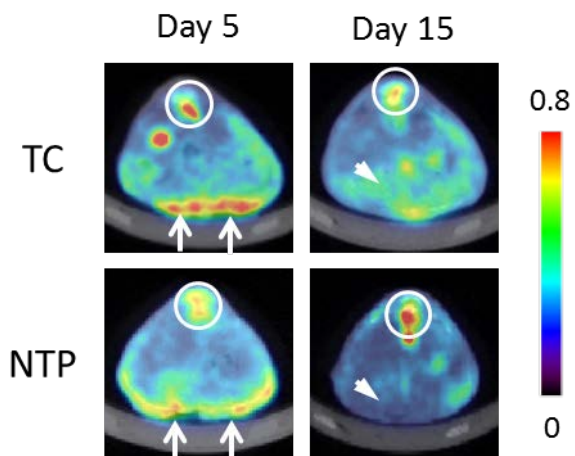


*Figure 4.* Representative PET/CT images of mice 2 h after injection of  $^{18}\text{F}$ -FDG. The vertebrae of mice are highlighted in white circles. The arrows and arrowheads indicate  $^{18}\text{F}$ -FDG accumulation in the laparotomy wound and the liver, respectively.

TC, thermal coagulator; NTP, non-thermal plasma.